J|A|C|S ARTICLES

Published on Web 08/26/2010

Furan Hydrogenation over Pt(111) and Pt(100) Single-Crystal Surfaces and Pt Nanoparticles from 1 to 7 nm: A Kinetic and Sum Frequency Generation Vibrational Spectroscopy Study

Christopher J. Kliewer,[†,‡] Cesar Aliaga,[†,‡] Marco Bieri,[†,‡] Wenyu Huang,[†,‡] Chia-Kuang Tsung,[†,‡] Jennifer B. Wood,[†,‡] Kyriakos Komvopoulos,[§] and Gabor A. Somorjai*[,†,‡]

Departments of Chemistry and Mechanical Engineering, University of California, Berkeley, California 94720, and Materials Sciences Division, Lawrence Berkeley National Laboratory, Berkeley, California 94720

Received July 1, 2010; E-mail: somorjai@socrates.berkeley.edu

Abstract: Sum frequency generation surface vibrational spectroscopy and kinetic measurements using gas chromatography have been used to systematically study the adsorption and hydrogenation of furan over Pt(111) and Pt(100) single-crystal surfaces and size-controlled 1.0-nm, 3.5-nm and 7.0-nm Pt nanoparticles at Torr pressures (10 Torr of furan, 100 Torr of H_2) to form dihydrofuran, tetrahydrofuran, and the ring-cracking products butanol and propylene. As determined by SFG, the furan ring lies parallel to all Pt surfaces studied under hydrogenation conditions. Upright THF and the oxametallacycle intermediate are observed over the nanoparticle catalysts under reaction conditions. Butoxy increases in surface concentration over Pt(111) with increasing temperature in agreement with selectivity trends.

1. Introduction

Catalytic reactions involving aromatic cyclic and heterocyclic molecules are important for the chemical industry for both fuel reforming and environmental concerns.[1] The adsorption of six-membered molecules, e.g. benzene and pyridine, has been extensively studied on various metal surfaces.[2−7] Five-membered ring systems, such as pyrrole, furan, and thiophene have received comparatively much less attention. This may be due in part to the more complex behavior of five-membered rings upon adsorption to catalytic surfaces, making them less attractive for fundamental surface science study. A thorough understanding of the adsorption and reactions of these five-membered aromatic molecules not only is important fundamentally as model systems for studying heterogeneous catalysis but also is directly important to the petrochemical industry as it applies to the hydrodenitrogenation, hydrodesulfurization, and hydrodeoxygenation processes.

The use of single crystals to study surface chemical reactions over metal catalysts has been a mainstay of surface science and catalysis research for many years,[8] and it provides the reference state needed to probe and compare more complex nanoparticle surfaces which are more closely related to what is used industrially. The technique of sum frequency generation vibrational spectroscopy, a surface specific vibrational spectroscopy, has proven to be a powerful surface analysis technique over single crystal catalysts to reveal both adsorption modes and reaction intermediates *in situ* from UHV to atmospheric reactant pressures.[6,9−15] SFG-VS has now been applied to the study of size-controlled nanoparticle systems,[16,17] which was not possible until recently due to the fact that the capping or stabilizing agent used in the synthesis of the nanoparticles interfered with the surface spectra of adsorbed reaction intermediates. However, Aliaga et al.[16] solved this problem by applying a UV−ozone cleaning treatment in the presence of oxygen to combust capping

[†] Department of Chemistry, University of California.
[‡] Lawrence Berkeley National Laboratory.
[§] Department of Mechanical Engineering, University of California.

(1) Cooper, B. H.; Donnis, B. B. L. *Appl. Catal., A* **1996**, *137*, 203.
(2) Netzer, F. P.; Bertel, E.; Matthew, J. A. D. *Surf. Sci.* **1980**, *92*, 43.
(3) Horsley, J. A.; Stohr, J.; Hitchcock, A. P.; Newbury, D. C.; Johnson, A. L.; Sette, F. *J. Chem. Phys.* **1985**, *83*, 6099.
(4) Ogletree, D. F.; Vanhove, M. A.; Somorjai, G. A. *Surf. Sci.* **1987**, *183*, 1.
(5) Weiss, P. S.; Eigler, D. M. *Phys. Rev. Lett.* **1993**, *71*, 3139.
(6) Bratlie, K. M.; Kliewer, C. J.; Somorjai, G. A. *J. Phys. Chem. B* **2006**, *110*, 17925.
(7) Kliewer, C.; Somorjai, G. *Catal. Lett.* **2010**, *137*, 118.
(8) Somorjai, G. *Introduction to Surface Science and Catalysis*; Wiley: New York, 1994.
(9) Cremer, P. S.; McIntyre, B. J.; Salmeron, M.; Shen, Y. R.; Somorjai, G. A. *Catal. Lett.* **1995**, *34*, 11.
(10) Cremer, P. S.; Su, X. C.; Shen, Y. R.; Somorjai, G. *J. Chem. Soc., Faraday Trans.* **1996**, *92*, 4717.
(11) Cremer, P. S.; Su, X. C.; Shen, Y. R.; Somorjai, G. A. *J. Am. Chem. Soc.* **1996**, *118*, 2942.
(12) Kliewer, C. J.; Bieri, M.; Somorjai, G. A. *J. Phys. Chem. C* **2008**, *112*, 11373.
(13) McCrea, K.; Parker, J. S.; Chen, P. L.; Somorjai, G. *Surf. Sci.* **2001**, *494*, 238.
(14) Buck, M.; Himmelhaus, M. *J. Vac. Sci. Technol., A* **2001**, *19*, 2717.
(15) Rupprechter, G.; Bruce, C. G.; Helmut, K. Sum Frequency Generation and Polarization-Modulation Infrared Reflection Absorption Spectroscopy of Functioning Model Catalysts from Ultrahigh Vacuum to Ambient Pressure. In *Advances in Catalysis*; Academic Press: 2007; Vol. 51, p 133.
(16) Aliaga, C.; Park, J. Y.; Yamada, Y.; Lee, H. S.; Tsung, C. K.; Yang, P. D.; Somorjai, G. A. *J. Phys. Chem. C* **2009**, *113*, 6150.
(17) Dellwig, T.; Rupprechter, G.; Unterhalt, H.; Freund, H. J. *Phys. Rev. Lett.* **2000**, *85*, 776.

 10.1021/ja105800z © **2010 American Chemical Society**

Scheme 1. Reaction for the Hydrogenation of Furan

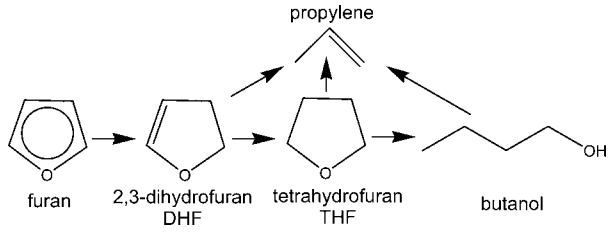

hydrocarbons from the surface of Pt nanoparticles deposited on a fused silica prism. In this study, this technique was applied so that the results over the single crystals could be compared to 1−7-nm platinum nanoparticles.

Furan (C_4H_4O) is a five-membered aromatic ring system (Scheme 1) in which one of the two lone pairs of electrons of the oxygen is delocalized over the π-system of the ring. The adsorption of furan on various single crystal surfaces has been studied. Sexton et al.[18] investigated the adsorption of furan on a Cu(100) surface using EELS and TDS determining that furan adsorbed to the surface at 85 K with a monolayer of furan molecules π-bonded and lying parallel to the surface, while a second "bilayer" builds on top of this which is tilted with respect to the surface. Gui et al.[19] studied the adsorption of the 5-membered heterocycles, including furan, on Pt(111) electrodes using EELS *ex-situ* after immersion in a solution of furan at a given pH. In this case the furan underwent hydrolysis on the Pt(111) surface. While the conditions are quite different than gas phase hydrogenation, it is interesting to note the ring-cracking over Pt(111). The adsorption structure of furan on Pd(111) was investigated by Knight et al.[20] using NEXAFS and scanned-energy mode photoelectron differaction (PhD), with the conclusion being that the furan molecule is adsorbed close to parallel (within 10°) to the Pd(111) surface. This is in agreement with STM images taken by Loui and Chiang[21] which demonstrate furan adsorbed nearly parallel to the Pd(111) surface. Solomon and Madix[22] determined both furan and dihydrofuran (DHF) adsorb to Ag(110) at a 22 ($\pm$ 7)° angle using NEXAFS.

Limited work has been performed over Pt surfaces as to the adsorption and reaction of furan. Hlavathy et al.[23] studied furan and tetrahydrofuran (THF) adsorption to a Pt foil using work function changes and Auger electron spectroscopy. Their determination was that furan adsorbs to a Pt foil via a surface π-complex, which would necessitate a near-parallel adsorption scheme. They determine further that THF is adsorbed to Pt via a C−Pt σ-bond and that the addition of hydrogen may increase C−O dissociation (bond scission) within the reactants.

The catalytic study of furan hydrogenation was first carried out in 1949 by Smith and Fuzek[24] over Adams platinum (platinum dioxide reduced in hydrogen). It was observed that furan hydrogenation yielded one product, butanol. By using kinetic arguments, it was argued that over Adams platinum the reaction mechanism proceeded along one of two pathways. The furan ring could hydrogenate to yield dihydrofuran and tetrahydrofuran sequentially, or the furan ring could break to form butanol once desorbed, but the conversion of DHF or THF to butanol was not observed.

In this study the hydrogenation of furan to form the observed products DHF, THF, and the ring-cracking products butanol and propylene (Scheme 1) was carried out over Pt(111) and Pt(100) single crystals to help elucidate the effect catalyst structure has on the reaction mechanism and selectivity, and these results are compared to the reaction carried out over 1.0-nm, 3.5-nm and 7.0-nm Pt nanoparticles to help determine the effect of catalyst size. Further, sum frequency generation vibrational spectroscopy was carried out *in situ* to elucidate the surface species over all of the model catalysts in the temperature range of 23 to 140 °C under 10 Torr of furan and 100 Torr of hydrogen.

2. Experimental Section

2.1. Materials. Prior to use, furan (>99%, Sigma-Aldrich), 2,3-dihydrofuran (99%, Aldrich), tetrahydrofuran (>99%,Sigma-Aldrich) and 1-butanol (99.8%,Sigma-Aldrich) were subjected to several freeze−pump−thaw cycles and the purities were checked by means of gas chromatography.

2.2. The High-Pressure/Ultrahigh-Vacuum System. All single crystal experiments reported here were carried out in a high-pressure/ultrahigh-vacuum (HP/UHV) system. The UHV chamber is operated at a base pressure of 2×10^{-10} Torr and is isolated from the HP cell by a gate valve. The UHV system is equipped with an Auger electron spectrometer (AES), a quadrupole mass spectrometer (Stanford Research Systems) and an ion bombardment gun (Eurovac). The HP cell consists of two CaF_2 conflat windows that allow transmission of infrared (IR), visible (VIS) and sum frequency radiation for sum frequency generation (SFG) experiments. The product gases in the HP cell are constantly mixed via a recirculation pump, and kinetic data is acquired by periodically sampling the reaction mixture and analyzing the relative gas phase composition in a flame ionization detector (FID) of a gas chromatograph (Hewlett-Packard HP 5890 on a 5% Carbowax 20 M packed column).

2.3. Single Crystal Sample Preparation. Prior to each experiment, the Pt(111) and Pt(100) crystal surfaces were cleaned in the UHV chamber by Ar^+ (1 keV for Pt) sputtering for 20 min at about 3×10^{-5} Torr of Ar. After sputtering, the crystals were heated to 1103 K in the presence of O_2 of 5×10^{-7} Torr and annealed at the same temperature for 2 min. The cleanliness of the crystal surfaces was verified by AES and the crystallographic structure verified with low energy electron diffraction (LEED). The samples were then transferred into the HP cell for SFG and kinetic studies.

2.4. Nanoparticle Preparation. The synthesis and characterization of the nanoparticles used in this study has been previously reported and is not the focus of this work[16,25−28] Further, the stability of the nanoparticles against agglomeration during the UV−ozone cleaning treatment has been previously reported.[16]

2.5. 7-nm Pt Cubic and 3.5-nm Nanocrystal Synthesis. A total of 0.05 mmol of Pt ion $(NH_4)_2Pt(IV)Cl_6$, 0.75 mmol of tetramethylammonium bromide, and 1.00 mmol of poly(vinylpyrrolidone) (in terms of the repeating unit; MW 29,000) were dissolved into 10 mL of ethylene glycol in a 25 mL round-bottom flask at room temperature. The mixed solution was heated to 180 °C in an oil bath at 60 °C/min. For 3.5 nm Pt spherical nanocrystal synthesis, a total of 0.05 mmol of Pt ion $(NH_4)_2Pt(II)Cl_4$), 0.75 mmol of

(18) Sexton, B. A. *Surf. Sci.* **1985**, *163*, 99.
(19) Gui, J. Y.; Stern, D. A.; Lu, F.; Hubbard, A. T. *J. Electroanal. Chem.* **1991**, *305*, 37.
(20) Knight, M. J.; Allegretti, F.; Kröger, E. A.; Polcik, M.; Lamont, C. L. A.; Woodruff, D. P. *Surf. Sci.* **2008**, *602*, 2524.
(21) Loui, A.; Chiang, S. *Appl. Surf. Sci.* **2004**, *237* (1−4), 555.
(22) Solomon, J. L.; Madix, R. J.; Stohr, J. *J. Chem. Phys.* **1991**, *94*, 4012.
(23) Hlavathy, Z.; Tetenyi, P. *Surf. Sci.* **2007**, *601*, 2026.
(24) Smith, H. A.; Fuzek, J. F. *J. Am. Chem. Soc.* **1949**, *71*, 415.
(25) Huang, W.; Kuhn, J. N.; Tsung, C. K.; Zhang, Y.; Habas, S. E.; Yang, P.; Somorjai, G. A. *Nano Lett.* **2008**, *8*, 2027.
(26) Kuhn, J. N.; Huang, W. Y.; Tsung, C. K.; Zhang, Y. W.; Somorjai, G. A. *J. Am. Chem. Soc.* **2008**, *130*, 14026.
(27) Lee, H.; Habas, S. E.; Kweskin, S.; Butcher, D.; Somorjai, G. A.; Yang, P. D. *Angew. Chem., Int. Ed.* **2006**, *45*, 7824.
(28) Zhang, Y. W.; Grass, M. E.; Kuhn, J. N.; Tao, F.; Habas, S. E.; Huang, W. Y.; Yang, P. D.; Somorjai, G. A. *J. Am. Chem. Soc.* **2008**, *130*, 5868.

tetramethylammonium bromide, and 1.00 mmol of poly(vinylpyrrolidone) (in terms of the repeating unit; M.W. 29,000) were dissolved into 10 mL of ethylene glycol in a 25 mL round-bottom flask at room temperature. The mixed solution was heated to 160 °C in an oil bath at 60 °C/min. The solutions were held at these respective temperatures for 20 min under argon protection and magnetic stirring, resulting in a dark brown solution. After the solution was cooled to room temperature, acetone (90 mL) was then added to form a cloudy black suspension, which was separated by centrifugation at 3,000 rpm for 10 min. The black product was collected by discarding the colorless supernatant. The products were further washed three times by precipitation/dissolution (redispersed in 20 mL of ethanol and then precipitated by adding 80 mL of hexanes). The nanocrystals were then redispersed in 10 mL of ethanol for characterization and catalyst preparation.

2.6. Synthesis of Dendrimer Templated NPs. Dendrimer encapsulated NPs were synthesized following a previously published method[25] with minor modifications. Generation 4 dendrimers (G4OH) were purchased from Dendritech Inc. (Midland, MI) as 10.2% (mass) methanol solution and used without further purification. A dendrimer stock solution (250 μM) was prepared by adding the dendrimer methanol solution to water. The dendrimer stock solution was mixed with 40 molar equiv of an aqueous solution of 0.01 M K_2PtCl_4 in a 20 mL vial. The vial was purged with Ar for 30 min, tightly sealed with a septum, and allowed 66 h for complexation. Then, a 20-fold excess of freshly prepared 0.5 M $NaBH_4$ (stored at 0 °C before use) was injected into the vial dropwise under vigorous stirring. The reaction solution was stirred for an additional 8 h. The reaction solution (10 mL) was purified by dialysis against 2 L of deionized water in cellulose dialysis sacks with a molecular weight cutoff of 12,000 (Sigma-Aldrich, Inc., St. Louis, MO). Dialysis occurred over 24 h with the water being changed 4 times. The average number of metal atoms per nanoparticle is controlled by the Pt ion to dendrimer ratio. Since the particles were too small to successfully image with TEM, sizes were calculated from the average number of metal ions added per dendrimer, and this method has been verified using X-ray absorption.[29] In this case approximately 40 Pt atoms were added to the dendrimer (Pt-40), creating a 1.0-nm Pt nanoparticle.

The 1.0-nm Pt nanoparticles were then drop cast onto a fused silica prism for catalytic and SFG-VS study. The 3.5-nm and 7-nm nanoparticles were deposited onto the fused silica prism using the Langmuir−Blodgett technique as described previously.[16] The particles were all UV−ozone treated on the fused silica prism[16] to remove the organic capping layer. The removal of the capping layer was verified by observing the disappearance of the C−H stretching vibrations in the SFG-VS spectrum.

2.7. Sum Frequency Generation Vibrational Spectroscopy. For SFG measurements, an active/passive mode-locked Nd:YAG laser (Leopard D-20, Continuum) with a pulse width of 20 ps and a repetition rate of 20 Hz was used. The fundamental output at 1064 nm was sent through an optical parametric generation/amplification (OPG/OPA) stage where a tunable IR (2300−4000 cm^{-1}) and a second harmonic VIS (532 nm) beam were created. The IR (150 μJ) and visible (200 μJ) beams were spatially and temporally overlapped on the crystal surface at angles of incidence of 55° and 60°, respectively, with respect to the surface normal for the single crystal studies. In the case of the nanoparticle studies, the beams were directed into a fused silica prism on top of which the nanoparticles had been deposited. The generated SFG beam was collected and sent through a motorized monochromator equipped with a photomultiplier tube to detect the SFG signal intensity. The signal-to-noise ratio was further increased by using a gated integrator while the IR beam was scanned through the spectral region of interest. The SFG process is enhanced when the IR beam comes into resonance with a vibrational mode of a molecule adsorbed at the surface, giving rise to a vibrational spectrum of adsorbed species. More information on the HP/UHV system and SFG measurement can be found elsewhere.[30−35]

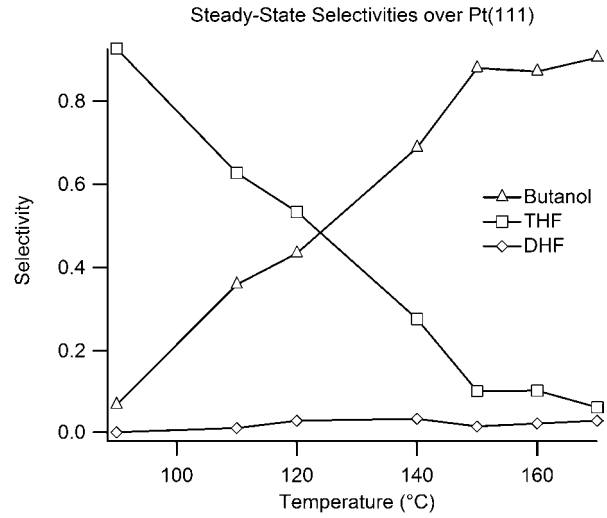

Figure 1. Temperature dependence of the selectivity during the hydrogenation of furan over Pt(111) using 10 Torr of furan and 100 Torr of hydrogen as measured by GC. The products are dihydrofuran (◇), tetrahydrofuran (□), and butanol (△). There is a complete selectivity reversal from 90 to 150 °C from tetrahydrofuran to the ring-cracking product butanol.

3. Results and Discussion

3.1. Furan Hydrogenation over Pt(111): Kinetic and SFG-VS Results. Furan hydrogenation was carried out over Pt(111) with 10 Torr of furan, 100 Torr of hydrogen, and 550 Torr of argon in the temperature range of 22 to 170 °C. Figure 1 displays the initial reaction product distribution as a function of temperature as measured by GC while the total conversion is less than 5%. Dihydrofuran, tetrahydrofuran and butanol were all detectable products. The catalytic activity of the high-pressure cell and sample holder was measured at all experimental temperatures used and found to be negligible. As can be seen, up to 90 °C the dominant product is THF, the saturated ring product. As the temperature is raised however, we see a complete reversal of the selectivity and the dominant product (~90%) becomes the ring-cracking product butanol. DHF is a minor product (<4%) at all temperatures. It is interesting to note that Smith and Fuzek[24] report only butanol as the reaction product over an Adams platinum catalyst while all three products are observed over Pt(111).

Figure 2 shows the SFG-VS spectrum of 10 Torr of furan over Pt(111) in the absence of excess hydrogen. Four major vibrational stretches are observed. The strongest two stretches are clearly seen at 2845 cm^{-1} and 2925 cm^{-1} corresponding to the CH_2 symmetric and asymmetric stretch of the THF ring respectively. It is possible that DHF on the surface could contribute to the CH_2 stretches as well. A third stretch is seen at 3145 cm^{-1} which we can attribute to the aromatic C−H

(29) Alexeev, O. S.; Siani, A.; Lafaye, G.; Williams, C. T.; Ploehn, H. J.; Amiridis, M. D. *J. Phys. Chem. B* **2006**, *110*, 24903.
(30) Bratlie, K. M.; Flores, L. D.; Somorjai, G. A. *Surf. Sci.* **2005**, *599*, 93.
(31) Kung, K. Y.; Chen, P.; Wei, F.; Rupprechter, G.; Shen, Y. R.; Somorjai, G. A. *Rev. Sci. Instrum.* **2001**, *72*, 1806.
(32) Yang, M. C.; Tang, D. C.; Somorjai, G. A. *Rev. Sci. Instrum.* **2003**, *74*, 4554.
(33) Shen, Y. R. *The Principles of Nonlinear Optics*; John Wiley & Sons: Hoboken, NJ, 2003.
(34) Shen, Y. R. *Annu. Rev. Phys. Chem.* **1989**, *40*, 327.
(35) Shen, Y. R. *Nature* **1989**, *337*, 519.

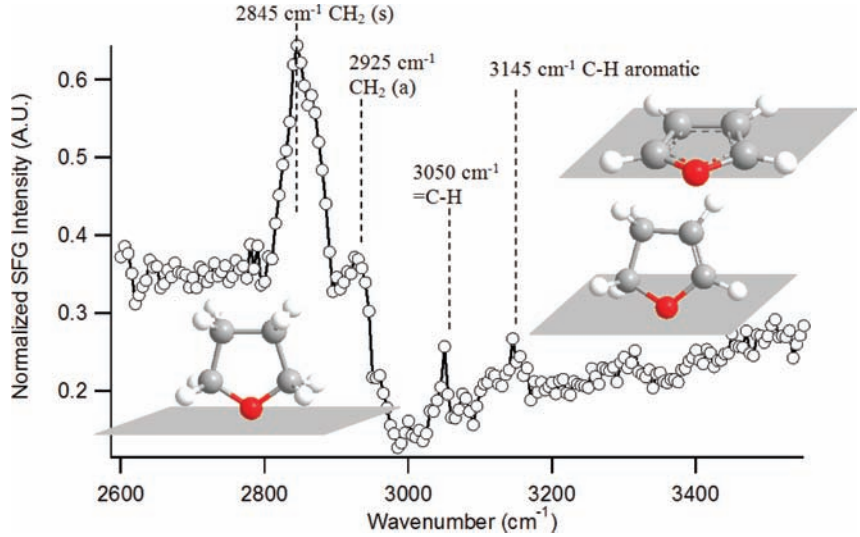

Figure 2. SFG-VS spectrum of 10 Torr of furan over Pt(111) in the absence of excess hydrogen taken at 23 °C. Stretches are seen for the C−H aromatic stretch of furan, the C−H vinylic stretch of DHF, and the CH_2 symmetric and asymmetric stretches of the THF ring. In the molecule representations, oxygen is red, carbon is gray, and hydrogen is white.

stretch of the furan ring. A thorough description of the vibrational modes of furan was done by Klots et al.,[36] and the gas phase aromatic C−H stretch of furan arises at 3160 cm^{-1}. Thus, a 15 cm^{-1} red-shift of this mode takes place upon the adsorption of furan to Pt(111). Lastly, a C−H stretch is observed at 3040 cm^{-1} which we assign to the vinylic C═C−H stretch of the DHF ring. Clearly, some hydrogenation is taking place on the surface species prior to the addition of excess hydrogen to the reaction mixture, although no detectable turnover was measured by GC. This could be due either to the small background pressure of hydrogen in the high-pressure cell or to intermolecular hydrogen transfer.

Figure 3 displays the temperature dependent spectra of 10 Torr of furan in the presence of 100 Torr of hydrogen over Pt(111). The spectra are characterized by three peaks at 2860 cm^{-1}, 2925 cm^{-1}, and 2960 cm^{-1}. The peak at 2860 cm^{-1} can be attributed to the CH_2(s) stretch of the saturated ring, THF. The peak at 2960 cm^{-1} is very clearly indicative of the CH_3(a) stretch of the ring-cracking product, butanol. The peak at 2925 cm^{-1} red-shifts to 2915 cm^{-1} upon heating and may be attributed to a CH_2(a) stretch. The CH_2(s) stretch seen at 2860 cm^{-1} is blue-shifted slightly from standard hydrocarbon CH_2(s) stretches, due to the electron withdrawing effects of the O atom in the molecule. Further, the dominance of the CH_2(s) stretch relative to the CH_2(a) stretch at 23 °C is indicative of a "standing up" THF species with respect to the metal surface.[37] No C−H aromatic stretch is seen once hydrogen is added to the reaction mixture, not even at room temperature when the gas phase is still >99.9% furan. This indicates that the furan ring is lying parallel to the Pt(111) surface upon the coadsorption of furan and hydrogen.

The three peaks undergo a general trend made clear by Figure 4 upon heating the crystal. In Figure 4 the spectrum of 10 Torr of furan and 100 Torr of hydrogen at 107 °C has been subtracted from the spectrum at 23° to highlight the trend observed as the crystal is heated to 107 °C. First, a very strong negative peak, or "loss peak", at 2860 cm^{-1} is seen. This occurs concomitantly

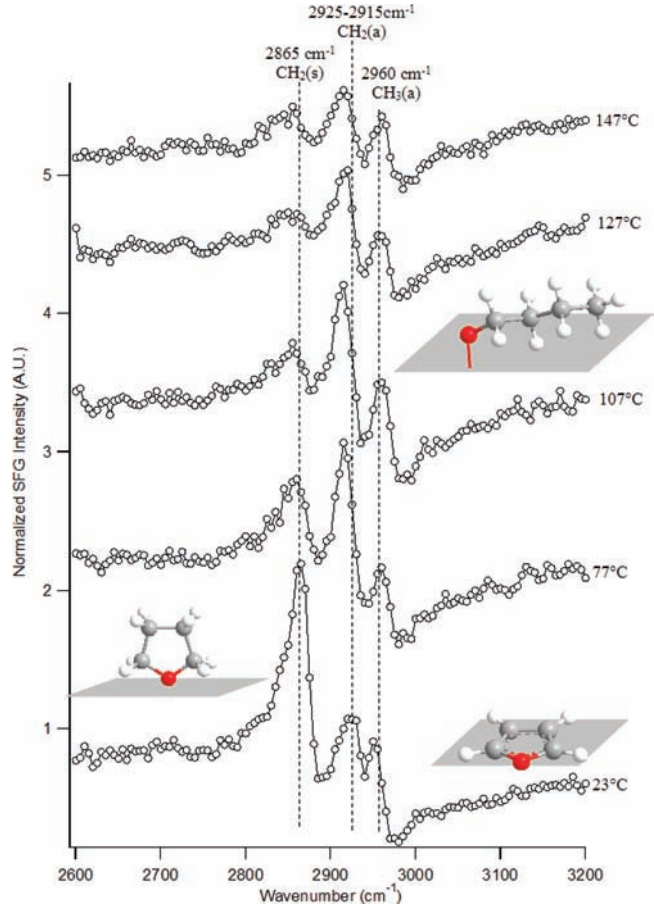

Figure 3. SFG-VS spectra of 10 Torr of furan and 100 Torr of hydrogen over Pt(111) from 23 to 147 °C.

with a gain in intensity at 2915 cm^{-1} and 2965 cm^{-1}. The gain observed in the peak at 2965 cm^{-1} can be attributed to an increasing surface concentration of butoxy, the ring-cracking product, with increasing temperature. Clearly, the desorption of the products is a rate limiting step for this reaction as the surface builds up an appreciable concentration. SFG-VS is not a suitable technique to quantify the relative surface coverages.

(36) Klots, T. D.; Chirico, R. D.; Steele, W. V. *Spectrochim. Acta, Part A* **1994**, *50*, 765.
(37) Yang, M.; Somorjai, G. A. *J. Am. Chem. Soc.* **2004**, *126*, 7698.

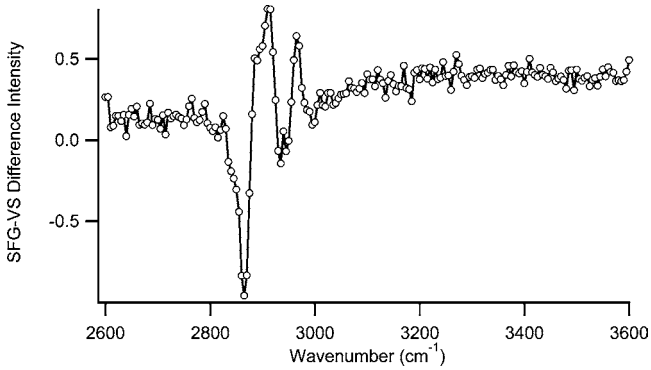

Figure 4. Difference spectrum of 10 Torr of furan and 100 Torr of hydrogen over Pt(111) at 107 °C as compared with 10 Torr of furan and 100 Torr of hydrogen at 23 °C to clarify the trends observed as the temperature is raised. A "loss" peak is observed at 2865 cm^{-1} upon heating corresponding to the CH_2 (s) stretch, while two positive peaks are seen at 2915 cm^{-1} and 2965 cm^{-1}.

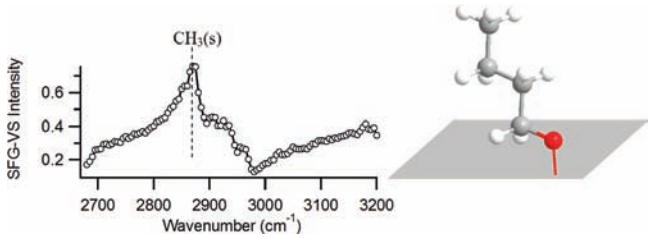

Figure 5. SFG-VS reference spectrum of 1 Torr of butanol over Pt(111) at 23 °C. The dominant CH_3(s) peak at 2875 cm^{-1} indicates that butanol adsorbs upright on the surface.

The presence of the methyl asymmetric stretch and the absence of the methyl symmetric stretch, which would appear at 2875 cm^{-1}, indicate that the butanol molecule is adsorbed to the surface with the chain parallel to the surface. Further, there is no evidence of an O−H bond anywhere in the 3200−4000 cm^{-1} range which leads us to conclude that butanol is adsorbed to the surface through an O−Pt bond, forming a butoxy species. Figure 5 displays the SFG-VS spectrum of 1 Torr of butanol over Pt(111) as a reference. As can be seen, without the presence of coadsorbates the spectrum for butanol on Pt(111) is dominated by the methyl symmetric stretch at 2875 cm^{-1} indicating that the molecular axis of the methyl must be aligned nearly perpendicular to the metal surface, and the methyl asymmetric stretch is very weak. No resonance in the O−H region was observable. This is in contrast to what is observed for the butoxy product on the Pt surface during the course of furan hydrogenation, for which the asymmetric methyl stretch is the visible one, indicating a different adsorption mode in the presence of coadsorbates such as furan and hydrogen on Pt(111).

The strong increase of the stretch observed at 2915 cm^{-1}, which occurs concomitantly as the 2865 cm^{-1} vanishes, has three possible interpretations. It may be due to the THF ring adsorption going from an "upright" geometry to a more "flat lying" geometry, due to the formation of an oxametallacycle intermediate as the ring cracks, or due to a parallel lying butoxy species on the surface with a gauche rotation (Figure 3). In the case of the oxametallacycle, the 2915 cm^{-1} stretch would be interpreted as the CH_2(s) stretch off of the C which is bound to the Pt surface (Figure 6). This type of shift in the symmetric stretch has been observed before with RAIRS[38] upon the formation of a C6 metallacycle on Pt(111) and appeared around ~2910 cm^{-1}. Over Ag(110), a 2 carbon oxametallacycle was

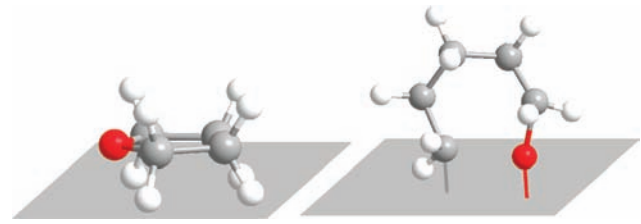

Figure 6. Two possible intermediates on Pt(111) during furan hydrogenation at 107 °C and higher. On the left is a parallel THF molecule, and on the right is an oxametallacycle.

prepared by thermally treating 2-iodoethanol, and resulted in a single band at 2922 cm^{-1}.[39] However, in the case of furan hydrogenation over Pt(111), one would expect to see a nearly equivalent peak intensity associated with the CH_2(s) stretch of the carbon connected to the oxygen (Figure 6), which is not observed as by 107−127 °C there is significantly more intensity at the 2915 cm^{-1} peak than at the 2865 cm^{-1} peak. Thus, the oxametallacycle intermediate cannot fully explain the spectrum.

In the case of the orientational change in the THF ring as the interpretation, the 2915 cm^{-1} peak would be attributed to the CH_2(a) stretch off of the THF ring. This is further evidenced in that the stretch red-shifts by 10 cm^{-1} upon heating, indicating more interaction with the metal surface. As the ring goes from more perpendicular to the surface to more parallel to the surface, we would expect the methylene symmetric stretch to vanish and the methylene asymmetric stretch to become dominant due to the metal surface selection rule. This is in agreement with the spectra.

Finally, as discussed above, the third interpretation is simply an increasing presence of gauche (GTT) butoxy bound to the surface as we raise the temperature. The presence of the asymmetric peak at 2965 cm^{-1} informs us that this is occurring on the surface to some extent.

Thus there are several conclusions from the interpretation of the SFG-VS results during furan hydrogenation on Pt(111). First, furan lies parallel to the Pt(111) surface during hydrogenation. Second, at 23 °C in the presence of 10 Torr of furan and 100 Torr of hydrogen we have predominantly an "upright" THF molecule on the surface. Third, butoxy is bound to the Pt(111) surface in the gauche (GTT) conformation growing in with temperature bound though the oxygen atom. Last, there may exist on the surface either an increasingly "parallel" lying THF species as the temperature is raised or an oxametallacycle, neither of which can be ruled out or completely verified by the acquired spectra in the available spectral range.

3.2. Furan Hydrogenation over Pt(100): Kinetics and SFG-VS. Figure 7 displays the steady state selectivity for furan hydrogenation over Pt(100) as a function of temperature for comparison to Pt(111) so as to help elucidate the effect that catalyst structure plays in this reaction. As can be seen, at 90 °C a nearly 50/50 product distribution is obtained between tetrahydrofuran and butanol. When compared to Pt(111) at 90 °C, it is evident that there is significantly more ring-cracking on the Pt(100) surface at lower temperatures than on the (111) face. As the temperature is raised to 160 °C, the selectivity becomes 86% for the cracking product butanol. This is the same general trend observed over Pt(111) in that butanol becomes

(38) Ilharco, L. M.; Garcia, A. R.; Hargreaves, E. C.; Chesters, M. A. *Surf. Sci.* **2000**, *459*, 115.
(39) Jones, G. S.; Mavrikakis, M.; Barteau, M. A.; Vohs, J. M. *J. Am. Chem. Soc.* **1998**, *120*, 3196.

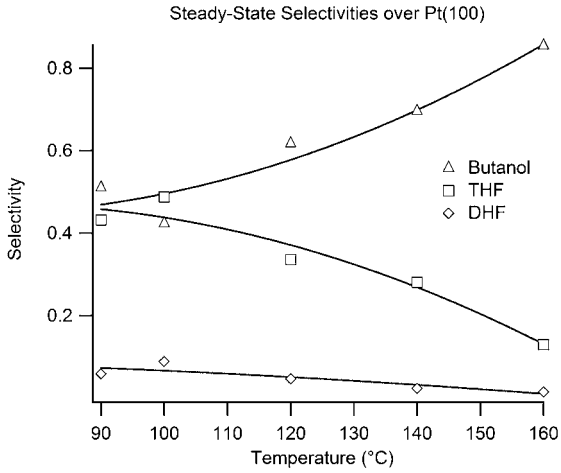

Figure 7. Steady state product distribution (selectivity) as a function of temperature on Pt(100) under 10 Torr of furan and 100 Torr of hydrogen. The products are dihydrofuran (◇), tetrahydrofuran (□), and butanol (△).

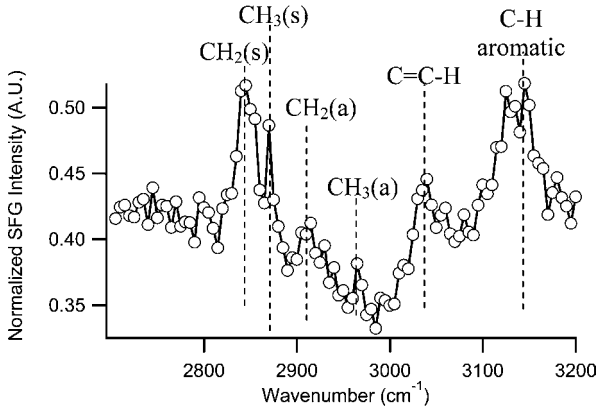

Figure 8. SFG-VS spectrum of 10 Torr of furan over Pt(100) at 23 °C. No excess hydrogen was added. Four resonances are seen. At 3145 cm^{-1} is the C−H aromatic stretch indicating a furan ring which is not parallel to the surface. At 3040 cm^{-1} is observed a vinylic C═C−H stretch of the partially saturated DHF ring. At 2915 cm^{-1} and 2850 cm^{-1} the methylene asymmetric and symmetric stretches are seen respectively. A narrow peak at 2870 cm^{-1} is seen which would correspond to the methyl symmetric stretch of the ring cracking product butanol.

the dominant product at high temperatures. The production of the partially saturated ring, which may be a desirable intermediate for synthetic applications, is very low as in the case over Pt(111). DHF is 8.9% of the product at 90 °C over Pt(100), and it is 0.9% of the product at 90 °C over Pt(111). Although it is a minor product, Pt(100) generates 10 times more DHF than Pt(111) at this temperature.

Figure 8 displays the SFG-VS spectrum of 10 Torr of furan over Pt(100) in the absence of excess hydrogen. At 3145 cm^{-1} a strong C−H aromatic stretch is seen for the furan ring, which is quite different from the very weak C−H aromatic stretch seen on Pt(111) under the same conditions. This indicates that the furan ring is significantly tilted upward with respect to the Pt(100) surface. A vinylic C═C−H stretch is observed at 3040 cm^{-1} corresponding to the vinylic portion of the partially saturated ring of dihydrofuran. The methylene symmetric and asymmetric stretches are observed at 2845 cm^{-1} and 2915 cm^{-1} respectively with the symmetric stretch significantly more dominant. The methyl symmetric and asymmetric stretches are also observed at 2870 cm^{-1} and 2965 cm^{-1} respectively, also exhibiting much stronger symmetric intensity. This spectrum

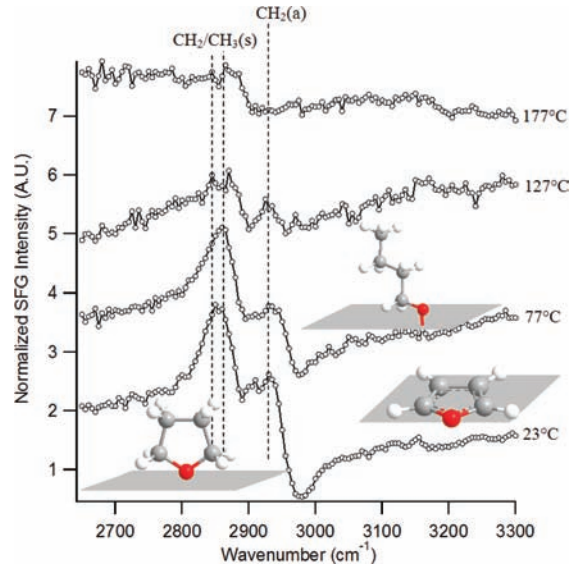

Figure 9. SFG-VS spectra of 10 Torr of furan and 100 Torr of hydrogen over Pt(100). The structures indicated are upright THF, upright butoxy, and parallel furan molecules.

implies that upon the adsorption of furan to Pt(100) at room temperature there exist vertically oriented furan, THF, DHF, and butoxy on the surface.

Figure 9 displays the spectra of 10 Torr of furan and 100 Torr of hydrogen over the Pt(100) surface as a function of temperature. Similarly to Pt(111) the aromatic and vinylic resonances disappear upon the addition of 100 Torr of hydrogen. This is an indication that under reactive conditions the furan ring lies parallel to the surface. The absence of the DHF peak may be due to a parallel orientation, but more likely due to this part of the reaction having a fast reaction rate constant forward to THF, i.e. the double bond is quickly hydrogenated. The methylene and methyl symmetric stretching vibrations are seen very close together at 2850 cm^{-1} and 2860 cm^{-1} at 23 °C, appearing as one wide peak with a doublet at the top. As the reaction mixture is heated to 127 °C however, the peaks resolve a little more and are seen at 2845 cm^{-1} and 2870 cm^{-1} respectively. By 147 °C nearly all resonant signal is lost with just a small peak seen at 2870 cm^{-1} for the methyl symmetric stretch, in agreement with an increased surface coverage of vertical butoxy. The methylene asymmetric stretch is seen at 2930 cm^{-1} while the methyl asymmetric stretch is not visible. These spectra indicate that both THF and butoxy are present on the surface in upright geometries (Figure 9) and as the surface is heated to 147 °C the adsorbates become less ordered generating less SFG-VS signal. The lack of a major peak around ∼2910 cm^{-1} rules out the presence of an oxametallacycle as a major surface species during furan hydrogenation over Pt(100). This does not eliminate the oxametallacycle as a transient intermediate between the ring and ring-cracked structures of furan and butanol, but if present it must nevertheless be short-lived enough as to not build up any appreciable surface concentration.

3.3. Furan Hydrogenation over Size-Controlled Pt Nanoparticles from 1.0 to 7.0 nm. To elucidate the effect that catalyst size has on this reaction, the hydrogenation of furan was also carried out over 1-nm, 3.5-nm and 7-nm Pt nanoparticles.

Figure 10 displays the reaction selectivity as a function of temperature during furan hydrogenation carried out over the three Pt nanoparticle sizes which had been UV−ozone cleaned

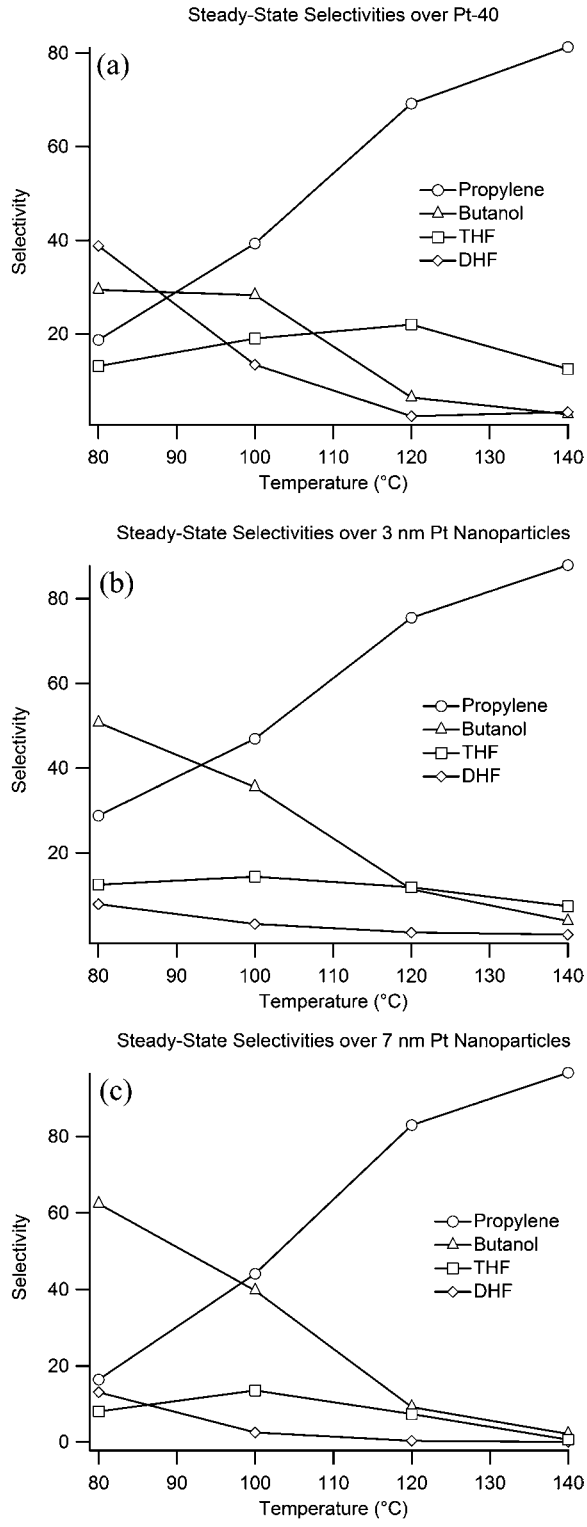

Figure 10. Product selectivities during furan hydrogenation on (a) 1.0-nm, (b) 3.5-nm, and (c) 7-nm Pt nanoparticles (10 Torr of furan, 100 Torr of hydrogen). The particles had been UV−ozone treated to remove the organic capping layer. The products are propylene (○), dihydrofuran (◇), tetrahydrofuran (□), and butanol (△).

until no C−H modes were present in the SFG-VS spectrum prior to reaction. A significant difference is seen in the product selectivities as compared with the single crystals. The partially saturated ring, DHF, was always a minor product over the single crystals, with Pt(100) having the highest selectivity of ∼9% at 90 °C. At 80 °C, the Pt-40 nanoparticles have a selectivity of

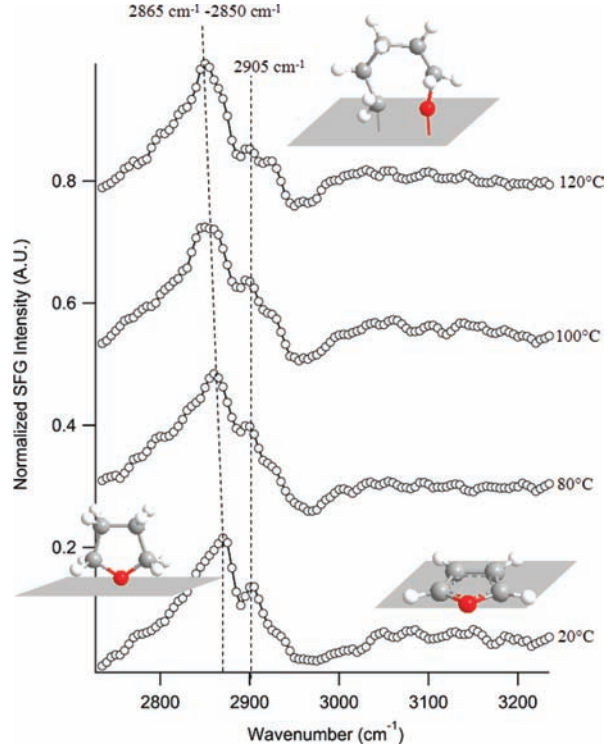

Figure 11. Temperature-dependent SFG-VS spectra acquired during furan hydrogenation (10 Torr of furan and 100 Torr of H_2) over Pt-40 nanoparticles.

39% for the formation of DHF. Butanol is always present in the product distribution, with a similar selectivity as that seen for the single crystals at lower temperatures, but as the temperature is raised the selectivity for butanol decreases as the formation of propylene becomes dominant over the three nanoparticle sizes studied. Propylene was not detected during furan hydrogenation over Pt(111) or Pt(100) and is unique to the nanoparticle catalysts. The production of propylene also indicates the formation of CO over the nanoparticle catalysts, which may act as a surface poison to the overall TOF over these catalysts. The GC column combination used to separate the larger products was not adequate to accurately characterize the CO production. The three nanoparticle sizes studied exhibited similar selectivity trends with temperature, as is seen in Figure 10.

Figure 11 displays the SFG-VS spectra of 10 Torr of furan and 100 Torr of hydrogen over a drop-cast film of the 1.0-nm Pt nanoparticles deposited onto a fused silica prism. Similarly to the single crystal results, no aromatic C−H stretch is observed indicating that the adsorbed furan is parallel to the nanoparticle surface. Only two vibrational resonances are observed. The first stretch, corresponding to the methylene symmetric mode of THF on the surface, is observed at 2865 cm^{-1} at room temperature and red-shifts to 2850 cm^{-1} by 120 °C. Again, the dominant symmetric stretch in combination with a very weak asymmetric stretch indicates an upright THF structure on the nanoparticle surface. The second mode appears at 2905 cm^{-1}, which corresponds to a highly perturbed CH_2(a) stretching mode consistent with the oxametallacycle intermediate as depicted in Figure 11.

Although propylene is a significant reaction product over the Pt nanoparticle catalysts, it is not observed as a surface species during reaction. Propylidyne is characterized[9] by a strong resonance at 2965 cm^{-1}, not observed in these spectra. The propyl intermediate exhibits two stretches below 2850 cm^{-1},

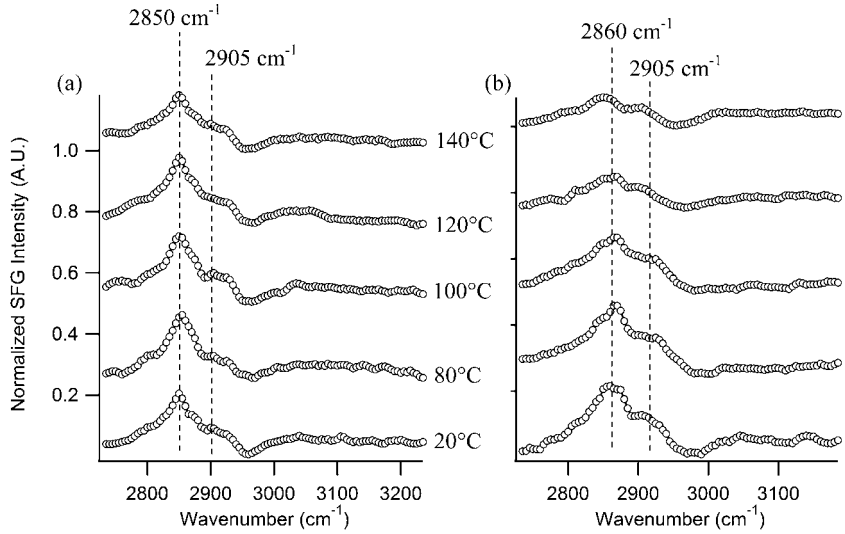

Figure 12. Temperature dependent SFG-VS spectra acquired during furan hydrogenation (10 Torr of furan and 100 Torr of H_2) over (a) 7-nm Pt nanoparticles and (b) 3.5-nm Pt nanoparticles.

and di-σ propylene adsorbed to the Pt surface gives a stretching mode at 2920 cm^{-1}. A broad peak centered at 3000 cm^{-1} is seen for π-bound propylene. As none of these characteristic features are seen, propylene is not adsorbed to the 1.0-nm Pt nanoparticle surface during furan hydrogenation indicating that desorption of propylene is rapid following molecular cracking on the surface.

Figure 12 displays the temperature-dependent SFG-VS spectra of furan hydrogenation over (a) 7.0-nm and (b) 3.5-nm Pt nanoparticles. The same two vibrational resonances are seen as over the 1.0-nm Pt nanoparticles, and the only difference is a slightly differing amount of red-shifting for the CH_2(a) mode. This is in agreement with the macroscopic selectivities observed for the furan hydrogenation reaction over the three nanoparticle sizes which exhibited very similar trends, much different than the results over Pt(111) and Pt(100). While Pt(111) and Pt(100) demonstrate both differing surface species as detected by SFG-VS and differing selectivities as detected by GC as a function of temperature, the nanoparticle catalysts all exhibit both similar surface-bound reaction intermediates and reaction selectivity trends when compared among the nanoparticle sizes.

4. Conclusions

In this study, sum frequency generation vibrational spectroscopy and gas chromatography have been applied to systematically study the surface species present on the Pt(111) and Pt(100) single crystal surfaces *in situ* during furan hydrogenation as well as the product selectivities as a function of catalyst temperature. These results are then compared to those obtained over UV−ozone cleaned Pt nanoparticles from 1.0 to 7.0 nm in size. The SFG-VS data indicates that on Pt(111) under furan hydrogenation conditions the planar furan ring lies parallel to the metal surface. Butanol is bound to the surface through the O atom, adsorbed in a gauche (GTT) orientation as the butoxy intermediate. The surface concentration of butoxy increases with increasing temperature over Pt(111), and THF is bound to the surface in an upright binding geometry. This was in agreement with the selectivity observed with GC over Pt(111) as the dominant product went from THF to butanol as the temperature was raised. Over Pt(100) the SFG-VS spectra also indicate a parallel furan adsorption under hydrogenation conditions. Both butoxy and THF are seen bound to the Pt(100) surface in upright geometries. The 1−7-nm Pt nanoparticles had upright THF and the oxametallacycle intermediate bound to the surface during reaction observed with SFG, and the nanoparticles exhibited a tendency toward further molecular cracking to form propylene in the gas phase observed by GC.

Acknowledgment. This work was supported by the Director, Office of Energy Research, Office of Basic Energy Sciences, and Materials Sciences Division of the U.S. Department of Energy under Contract DE-AC02-05CH11231. M.B. thanks the Swiss National Science Foundation (SNF) for financial support.

JA105800Z